

Time-stretched sampling of a fast microwave waveform based on the repetitive use of a linearly chirped fiber Bragg grating in a dispersive loop

JIEJUN ZHANG AND JIANPING YAO*

Microwave Photonics Research Laboratory, School of Electrical Engineering and Computer Science, University of Ottawa, Ontario K1N 6N5, Canada

*Corresponding author: jpyao@eecs.uottawa.ca

Received 21 March 2014; revised 28 May 2014; accepted 29 May 2014 (Doc. ID 208550); published 1 August 2014

Conventional sampling techniques may not be able to meet the ever-increasing demand for increased bandwidth from modern communications and radar signals. Optical time-stretched sampling has been considered an effective solution for wideband microwave signal processing. Here, we demonstrate a significantly increased stretching factor in the photonic time-stretched sampling of a fast microwave waveform. The microwave waveform to be sampled is intensity modulated on a chirped optical pulse generated jointly by a mode-locked laser and a length of dispersion compensating fiber. The pulse is then injected into an optical dispersive loop that includes an erbium-doped fiber amplifier and is stretched by a linearly chirped fiber Bragg grating multiple times in the loop. A record stretching factor of 36 is achieved based on an equivalent group delay dispersion coefficient of 12,000 ps/nm. This result could help address the new challenges imposed on signal processors to operate at a very high sampling rate. © 2014 Optical Society of America

OCIS codes: (060.7140) Ultrafast processes in fibers; (070.1170) Analog optical signal processing; (060.5625) Radio frequency photonics; (130.2035) Dispersion compensation devices.

<http://dx.doi.org/10.1364/OPTICA.1.000064>

1. INTRODUCTION

The ever-increasing bandwidth of modern communications and radar signals has imposed new challenges on signal processors to operate at a very high sampling rate. The use of the conventional sampling techniques may not be able to meet the demand. To realize broadband sampling, a solution is to use photonic-assisted sub-Nyquist sampling. Numerous approaches have been proposed, such as optical downsampling [1,2], optical undersampling [3], optical pseudorandom sampling [4], compressive sampling [5], and optical time-stretched sampling [6–14]. Among these techniques, optical time-stretched sampling has been considered an effective solution for wideband microwave signal processing.

In an optical time-stretched sampling system, a microwave waveform is modulated on a predispersed optical pulse, which,

after the modulation, travels through another dispersive element for time stretching. The second dispersive element should have a much greater group delay dispersion (GDD) coefficient than the first element. A time-stretched microwave waveform will be generated when the pulse is sent to a photodetector (PD) and a slow version of the original waveform is obtained [15]. This technique was first proposed by Coppinger *et al.* in [7], demonstrating a sampling rate that is 1/3.25 of the Nyquist frequency. Since then, new efforts have been dedicated to further reducing the sampling rate by increasing the stretching factor. In [8], dispersion-based time-stretched sampling with a stretching factor of 5 combined with compressive sensing was demonstrated to achieve a sampling rate as low as only 1/40 of the Nyquist frequency. The sampling rate is then further reduced to 1/80 of the Nyquist frequency by

using a time-stretched sampling module with a time stretching factor of 20 [9]. In [10], time-stretched sampling using a coherent receiver to improve the detection sensitivity by cancelling the dispersion-induced impairments and optical nonlinearity was demonstrated. A stretching factor of 24 was achieved by using two dispersive elements with two GDD coefficients of 45 and 1045 ps/nm for predispersion and time stretching, respectively. In [11], time-stretched sampling of a continuous-time signal was demonstrated based on virtual time gating, where a stretching factor of 1.5 was achieved. To overcome the “big data” problem associated with time-stretched sampling, Asghari and Jalali demonstrated a sampling solution based on nonlinear time stretching [12]. An equivalent stretching factor of 200 was achieved. The system has been further enhanced to achieve a real-time bandwidth suppression factor of 500 [13]. In the system, a programmable optical filter was used to modulate the microwave waveform to the optical pulse, which may make the system complicated and costly. In [14], an unprecedented time-stretching factor of 250 was realized by using a predispersion element with a GDD coefficient of 41 ps/nm and a double-pass dispersive element with a GDD coefficient of $-10,246$ ps/nm. To achieve such a large dispersion, an extremely long dispersion compensating fiber (DCF) is used. To compensate for the loss in the long DCF, four stimulated Raman amplifiers pumped by four high-power laser diodes were employed. Although the system could realize an effective sampling rate of 10 T samples/s, the use of a long DCF and multiple Raman amplifiers makes the system rather bulky and complicated. For a time-stretching element with a fixed GDD coefficient, to achieve a large stretching factor, the predispersion element could be selected to have a relatively small GDD coefficient. The consequence of using a predispersion element with small dispersion is that the input optical pulse cannot be sufficiently prestretched to have a large time duration, to allow a microwave waveform with a long duration to be modulated on the prestretched input pulse. Therefore, the fundamental solution for having a large stretching factor for a long-duration microwave waveform is to use a time-stretching element with a large GDD coefficient.

In fiber optics, a dispersive element can be a single-mode fiber (SMF), a DCF, or a linearly chirped fiber Bragg grating (LCFBG). Since an SMF has a relatively small dispersion coefficient, it is rarely used in a time-stretched sampling system, especially as the time-stretching dispersive element. A DCF, on the other hand, can have a dispersion coefficient that is several times greater than that of an SMF. However, to achieve large time stretching, a DCF with a length of several tens [10] or even hundreds [14] of kilometers is required. Thus, the system is still bulky and lossy. An LCFBG has been proved to be a highly effective dispersive element with low insertion loss and small nonlinear effects [16,17]. The GDD of an LCFBG is proportional to its grating length and inversely proportional to its bandwidth. For time-stretching applications, the bandwidth of an LCFBG is usually controlled to be equal to the bandwidth of the optical pulse. Hence, to have a large GDD coefficient, an LCFBG with a long length is needed. For example, a 10 cm long LCFBG with 1 nm bandwidth has a GDD coefficient of 1000 ps/nm. To further increase

the GDD coefficient, the length of the LCFBG should be further increased. Although an LCFBG with a length greater than 1 m is commercially available, the size is large and the fabrication is complicated and costly.

The use of a microwave waveguide with a large GDD coefficient has been explored in the past few years for spectrum analysis [18,19]. Recently, it was demonstrated [20] that by forming a dispersive loop that incorporates a microwave dispersive element and a microwave amplifier, an equivalent microwave dispersive element with a GDD coefficient that is several times greater than that of the original dispersive element can be achieved by recirculating the microwave waveform in the loop. Compared with a simple cascade of multiple dispersive elements for achieving an equivalent dispersive element with a large GDD coefficient, the recirculating dispersive loop has advantages such as a smaller device footprint, lower insertion loss, and a better signal-to-noise ratio (SNR) [20]. The major limitations of an electrical dispersive loop are the small bandwidth, usually below 1 GHz, and high loss. In addition, the maximum time delay is limited, although the constant time delay provided by a coaxial cable is already much larger compared to that of a waveguide. To implement a dispersive loop with a large GDD coefficient over a large bandwidth, a solution is to use photonic components. In addition to a broad bandwidth, an optical dispersive loop can generate a much longer time delay, since a long loop is possible due to the extremely low loss of an optical fiber. A time-stretched sampling system using an optical dispersive loop can significantly increase the stretching factor over a broad bandwidth.

In this paper, we propose a novel technique for achieving time-stretched microwave sampling with a significantly increased stretching factor. In the proposed system, a microwave waveform is modulated on a predispersed optical pulse, which is sent to a recirculating dispersive loop consisting of an LCFBG and an erbium-doped fiber amplifier (EDFA). The LCFBG is used to achieve repetitive pulse stretching, and the EDFA is used to compensate for the loss in the loop. By controlling the gain of the EDFA to compensate for the loop loss, the optical waveform can recirculate in the loop, and repetitive use of the LCFBG for accumulated pulse stretching is realized. The proposed technique is experimentally demonstrated. An LCFBG with a GDD coefficient of 1500 ps/nm is fabricated and incorporated in the recirculating dispersive loop. An equivalent GDD coefficient of 12,000 ps/nm is achieved, which, to the best of our knowledge, is the largest dispersion ever reported for time-stretched sampling. The corresponding stretching factor is 36. The use of the system to sample a microwave waveform is demonstrated. For a sampling system with a bandwidth of 32 GHz, the use of the proposed recirculating dispersive loop can extend the bandwidth by 36 times, or 1.15 THz (or a time resolution of 347 fs), with a frequency resolution of 4.93 GHz.

2. PRINCIPLE

The schematic of the proposed time-stretched sampling system is shown in Fig. 1. An optical pulse from a mode-locked laser (MLL) is sent to a DCF serving as a predispersion element.

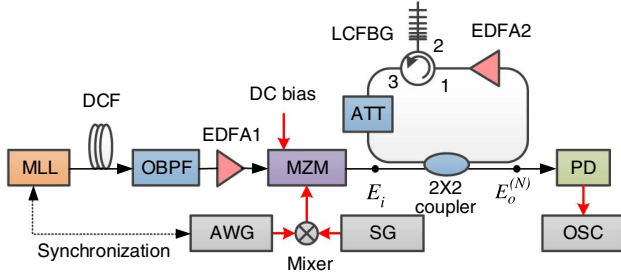


Fig. 1. Schematic of the time-stretched sampling system. MLL, mode-locked laser; OBPF, optical bandpass filter; DCF, dispersion compensating fiber; EDFA, erbium-doped fiber amplifier; MZM, Mach-Zehnder modulator; ATT, attenuator; LCFBG, linearly chirped fiber Bragg grating; PD, photodetector; AWG, arbitrary waveform generator; SG, signal generator; OSC, oscilloscope.

The predispersed optical pulse is then sent to a Mach-Zehnder modulator (MZM) through an optical bandpass filter (OBPF) and an EDFA (EDFA1). A microwave waveform is modulated on the predispersed optical pulse at the MZM. The modulated signal is then sent to the recirculating dispersion loop, in which an LCFBG and a second EDFA (EDFA2) are incorporated. Note that the bandwidth of the OBPF is identical to the bandwidth of the LCFBG, so the predispersed optical pulse at the output of the OBPF has a spectral width that is identical to that of the LCFBG. The microwave waveform to the MZM is generated by mixing an electrical gate signal from an arbitrary waveform generator (AWG) with a sinusoidal microwave signal from a microwave generator (SG). The modulated waveform is launched into the recirculating dispersive loop through a 2×2 3 dB coupler. In the loop, the LCFBG is used as a dispersive element and EDFA2 is used to compensate for the round-trip loss. An attenuator (ATT) is also included in the loop to provide fine control of the loop gain in order to maintain full compensation of the loss while avoiding optical lasing in the loop. The optical pulse is recirculating in the dispersive loop. The time-stretched optical pulse at the output of the loop is sent to a PD. The stretched microwave waveform is sampled by a real-time oscilloscope.

It is known that an LCFBG has a quadratic phase response within its passband. Its transfer function can be written as [21]

$$H_{\text{LCFBG}}(\omega) = \exp\left(-j\frac{\beta_C}{2}\omega^2\right), \quad (1)$$

where ω is the optical angular frequency and β_C is the GDD coefficient of the LCFBG (in ps^2). Assuming that the optical spectrum at the input of the dispersive loop is $E_i(\omega)$, the output spectrum after recirculating for N round trips in the loop can be written as

$$E_o^{(N)} = \left(\frac{\sqrt{2}}{2}\right)^{N+1} g^N E_i(\omega) H^N(\omega), \quad (2)$$

where g is the net gain of the loop, which can be changed by tuning the gain of EDFA2 or the loss of the attenuator. If we make g close to but slightly less than $\sqrt{2}$, we then have

$(\sqrt{2}g/2)^N \approx 1$. The transfer function of the loop can be expressed as

$$H_{\text{loop}}(\omega) = \frac{E_o^{(N)}}{E_i} = \frac{\sqrt{2}}{2} \exp\left(-j\frac{N\beta_C}{2}\omega^2\right). \quad (3)$$

By comparing Eqs. (1) and (3), we can see that the recirculating dispersive loop acts as a dispersive element that has an equivalent GDD coefficient of $N\beta_C$. It should be noted that in practice, $\sqrt{2}g/2$ should always be smaller than unity to prevent the loop from lasing. As a result, the amplitude of $H_{\text{loop}}(\omega)$ should decay with the increase of N . The maximum number of N is determined by the minimum SNR required to detect the time-stretched signal. If the 2×2 coupler is replaced by an optical switch, then the number of recirculations can be controlled by the optical switch. In this case, the equivalent GDD coefficient of the recirculating dispersive loop can be tunable by letting the waveform recirculate in the loop for a certain number of round trips.

The stretching factor of the time-stretched sampling system is given by

$$M = 1 + N\beta_C/\beta_D, \quad (4)$$

where β_D is the GDD coefficient of the predisposition element. Since the second term in Eq. (4) is much greater than 1, it can be seen that the stretching factor increases proportionally to the number of the round trips N . Again, if an optical switch is employed in the system, the stretching factor can then be adjusted to improve the performance of the sampling system according to the frequency band of the input waveform. For example, N should be large for a fast microwave waveform so that all the details of the microwave waveform can be revealed, while for a relatively slow microwave waveform, N should be small to avoid oversampling and data redundancy [12,13].

3. EXPERIMENT

An experiment based on the setup shown in Fig. 1 is performed. In the experiment, an MLL (IMRA femtolite 780) with a repetition rate of 48 MHz and a central wavelength of 1558 nm is employed to produce an optical pulse train. An individual pulse in the pulse train is nearly transform limited with a 3 dB spectral bandwidth of 8 nm. The predisposition element is a DCF with a dispersion coefficient of $\beta_C = 432 \text{ ps}^2$ (or -339 ps/nm). The LCFBG used in the dispersive loop has a dispersion coefficient of $\beta_C = 1912 \text{ ps}^2$ (or -1500 ps/nm) within a reflection passband of 0.6 nm centered at 1558 nm. The OBPF (Finisar WaveShaper 4000S) is configured to have a near-rectangular passband with a bandwidth identical to that of the LCFBG. It can be calculated that after the predisposition by the DCF and the filtering by the OBPF, the MLL pulse is stretched to have a time duration of $\Delta\tau = 203 \text{ ps}$. The optical pulse train at the output of the OBPF is amplified by EDFA1 and sent to the MZM. The MZM has a bandwidth of 20 GHz and is biased at its minimum transmission point. A microwave waveform generated by mixing an 18 GHz microwave signal from the

SG with a rectangular pulse train with a repetition rate of 286 kHz serving as a gate signal from the AWG is applied to the MZM. The repetition rate of the rectangular pulse train is smaller than that of the MLL (48 MHz) to reduce the duty cycle of the modulated optical pulse train, thus allowing pulse stretching with a large stretching factor without creating overlap between adjacent pulses. Note that in the experiment, the AWG and the MLL are synchronized. The modulated optical waveform at the output of the MZM is sent to the recirculating dispersive loop via the 2×2 coupler. The length of the recirculating dispersive loop is estimated to be 61 m (corresponding to a time delay of 305 ns). The time-stretched optical pulse from the recirculating dispersive loop is sent to the PD (25 GHz, New Focus). The electrical waveform at the output of the PD is sampled by a real-time oscilloscope (Agilent DSO-X 93204A).

The modulation process is depicted in Fig. 2. As can be seen from Fig. 2(a), the gate signal with a repetition rate of 286 kHz and a gate duration of 20.8 ns is mixed with the 18 GHz microwave generated by the SG and sent to the MZM. Since the MZM is biased at its minimum transmission point, the pre-dispersed pulse train corresponding to the low voltage level of the modulation waveform will not be able to pass through the MZM, and the pre-dispersed pulse train corresponding to the high voltage level of the modulation waveform is modulated by a microwave waveform with twice the frequency of the microwave signal generated by the SG (i.e., 36 GHz), as shown in Fig. 2(b). Therefore, the number of microwave cycles in each MLL pulse is 7. In addition, there will be only one MLL pulse that is modulated by the microwave waveform in every period of the gate. The resulting pulse train with a reduced repetition rate is illustrated in Fig. 2(c). It should be noted that for practical applications one can use an MLL with a lower repetition rate so that the gate signal is not needed. Then the MZM can be biased at the quadratic point and the waveform carried by the MLL pulse will be the same as the modulation signal.

The modulated pulses are then injected into the recirculating dispersive loop. In every round trip, part of the optical

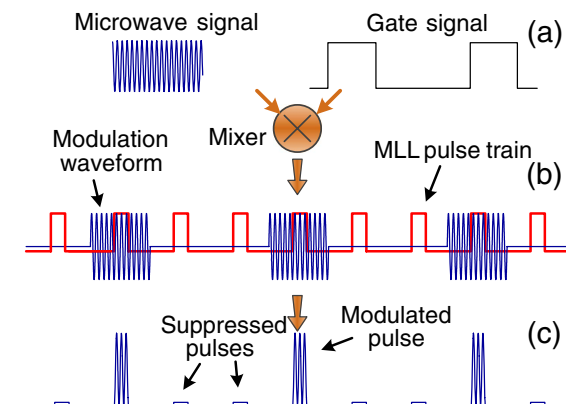


Fig. 2. Modulation process. (a) An 18 GHz microwave signal generated by the SG (solid blue line) and a gate signal generated by the AWG (black), (b) the waveform applied to the MZM (blue) and the MLL pulse train after predispersion and filtering (red), (c) the resulting optical pulse train carrying the microwave waveform with a reduced repetition rate.

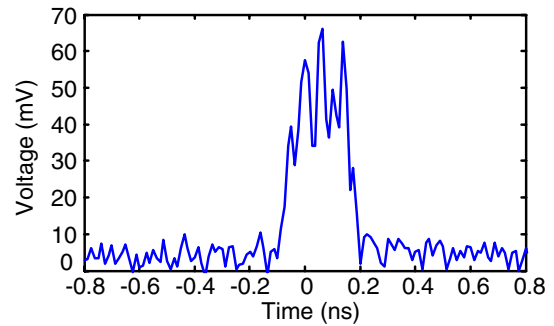


Fig. 3. Waveform of the modulated MLL pulse measured at the output of the MZM.

pulse is coupled out of the loop by the 2×2 coupler and detected by the PD.

Figure 3 shows the measured MLL pulse at the output of the MZM. The FWHM of the pulse is measured to be around 230 ps. Compared to the theoretical pulse width of $\Delta\tau = 203$ ps, the 27 ps difference could be caused by the relatively large sampling interval of 12.5 ps of the oscilloscope. The microwave waveform modulated on the pre-dispersed pulse cannot be correctly sampled, since the doubled microwave frequency of 36 GHz exceeds the highest frequency of the oscilloscope.

The waveform at the output of the dispersive loop is then measured by the real-time oscilloscope, as shown in Fig. 4. As can be seen when a modulated optical waveform is launched into the recirculating dispersive loop, a pulse burst with a decaying amplitude is generated. The quick decay in amplitude is due to the loss in the loop. To avoid lasing in the loop, the gain of EDFA2 is controlled to be smaller than the loss. The time duration between two adjacent pulses is 308 ns, which corresponds to the time delay of the recirculating dispersive loop. The time duration between two large pulses is 3.5 μ s, corresponding to the repetition time of the optical pulse train at the output of the MZM.

Theoretically, the decaying can be reduced by increasing the loop gain. However, due to the uneven magnitude response of the LCFBG and the uneven gain spectrum of EDFA2, the recirculating dispersive loop may start lasing at a certain wavelength when the loop gain is increased, while at the other wavelengths, the loop gain is still smaller than 1. The relatively high noise floor is mainly caused by the amplified spontaneous

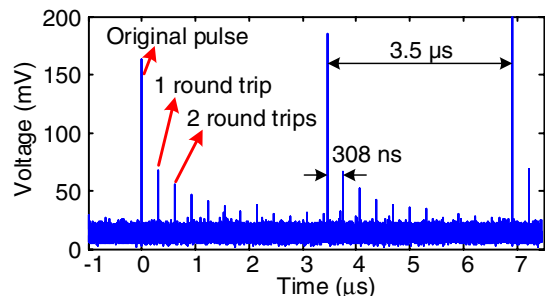


Fig. 4. Measured optical waveform at the output of the recirculating dispersive loop.

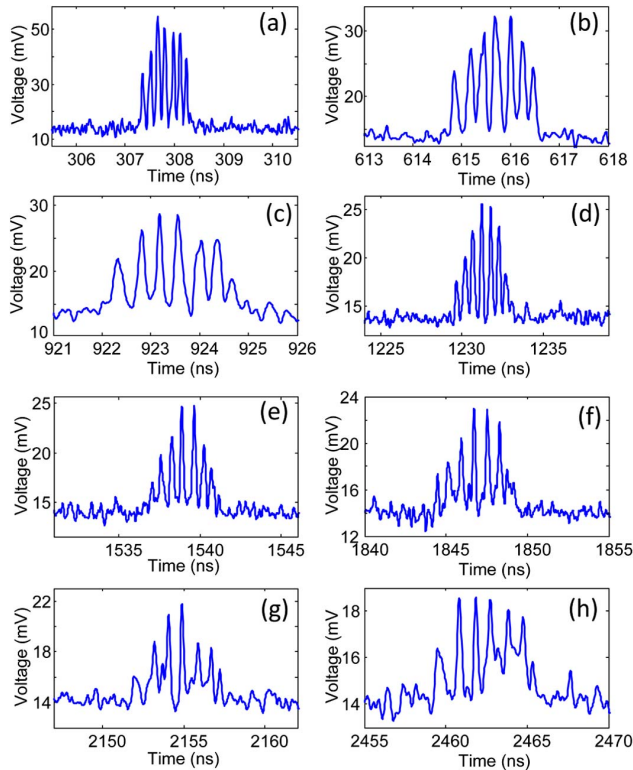


Fig. 5. Output waveforms after different numbers of round trips. (a) One round trip, (b) two round trips, (c) three round trips, (d) four round trips, (e) five round trips, (f) six round trips, (g) seven round trips, and (h) eight round trips. Note that the time scale is 1 ns/division in (a)–(c) and 5 ns/division in (d)–(h).

emission of EDFA2 and the occasional lasing of the loop, as the loop gain is very close to 1 at some wavelengths. To increase the SNR of the system, an LCFBG with a specially designed amplitude response or an EDFA gain-flattening filter should be included in the loop to avoid lasing. One may also use an optical switch to replace the optical coupler so that the loop loss can be reduced, and a lower gain for EDFA2 is required.

The detailed waveforms after the pulse is stretched in the recirculating dispersive loop for one to eight round trips are shown in Figs. 5(a)–5(h). After one round trip, the pulse duration is stretched to around 1 ns and all seven microwave cycles with a temporal separation between two adjacent cycles of around 140 ps can be identified, as shown in Fig. 5(a). The optical pulse is stretched with a stretching factor of around 5.

Then, the optical pulse keeps on recirculating in the loop, with the stretched pulses shown in Figs. 5(b)–5(h). Since the round-trip loss cannot be completely compensated by the gain of EDFA2, and the amplified spontaneous emission of EDFA2 introduces a significant amount of noise, the SNR drops after each round trip. By fine control of the loop gain using the tunable attenuator, we are able to make the pulse circulate for eight round trips before it is fully imbedded in the noise. For the pulse after the eighth round trip, the equivalent GDD is $8 \times 1500 \text{ ps/nm} = 12,000 \text{ ps/nm}$. The measured waveform after the eighth round trip shows that the pulse duration is around 7 ns and the average temporal separation between

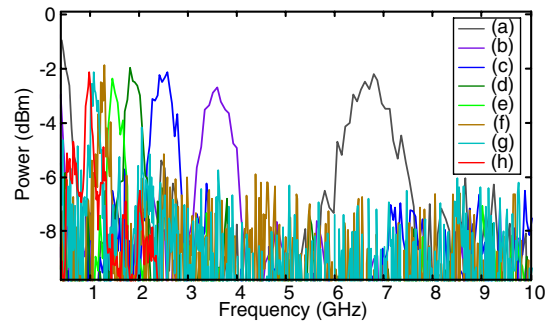


Fig. 6. Electrical spectra of the measured time-stretched waveforms for different numbers of round trips. (a)–(h) correspond to the waveforms given in Figs. 5(a)–5(h).

each microwave cycle is 1 ns. This indicates that a stretching factor of 36 is obtained, which is close to the theoretically calculated stretching factor of 36.4 based on Eq. (4). Assuming that the bandwidth of the system is limited by the oscilloscope used in our experiment, which is 32 GHz, the bandwidth of the sampling system can be as large as $36 \times 32 = 1.15 \text{ THz}$, corresponding to a time resolution of 347 fs. The frequency resolution, on the other hand, is limited by the time duration of the optical pulse used to carry the microwave waveform, which is $(203 \text{ ps})^{-1} = 4.93 \text{ GHz}$.

Figure 6 shows the electrical spectra of the measured waveforms for different numbers of round trips given in Fig. 5. The spectra show that the SNR decreases as the number of round trips increases, which agrees with our discussion. It can also be seen that for a single frequency input, there is only one output frequency component, which means that the signal distortion effect usually encountered by a time-stretched system has a weaker effect compared to the SNR deterioration and is negligible.

4. DISCUSSION AND CONCLUSION

A novel time-stretched sampling system with a large stretching factor has been demonstrated by the repetitive use of an LCFBG in a recirculating dispersive loop. An equivalent GDD as large as 12,000 ps/nm with a large stretching factor of 36 was achieved. This is the second largest dispersion-based stretching factor for a time-stretched sampling system ever reported. Although the stretching factor of 250 reported in [14] is much greater than the stretching factor of 36 in this work, we have demonstrated a dispersive element with a greater dispersion than that in [13]. If we used a predispersion element that has a similar dispersion coefficient as the one in [14], we would be able to achieve a much greater stretching factor than 250. Note that for pulse stretching with a very large stretching factor, the input pulse applied to the MZM should be very short; thus the system can only sample a microwave waveform with a narrow width.

It should also be noted that the stretching factor can be further increased by using a low-noise optical amplifier. In addition, by flattening the magnitude response of the LCFBG and the gain of EDFA2, the net gain in the loop can be controlled to be very close to 1, but with no lasing; thus an input

pulse can recirculate in the loop more times, which would lead to a much greater stretching factor. In [22], a microwave photonic filter with an ultra-even magnitude response was used to achieve pulse recirculation in an active cavity for 270 round trips. If this can be realized for a wideband LCFBG, the equivalent GDD can be as large as 4.05×10^5 ps/nm, which corresponds to a stretching factor of 1195.

FUNDING INFORMATION

China Scholarship Council (201206160086); Natural Sciences and Engineering Research Council of Canada (NSERC).

REFERENCES

1. P. W. Juodawlkis, J. J. Hargreaves, R. D. Younger, G. W. Titi, and J. C. Twichell, "Optical down-sampling of wide-band microwave signals," *J. Lightwave Technol.* **21**, 3116–3124 (2003).
2. B. C. Pile and G. W. Taylor, "Performance of subsampled analog optical links," *J. Lightwave Technol.* **30**, 1299–1305 (2012).
3. A. Feldster, Y. P. Shapira, M. Horowitz, A. Rosenthal, S. Zach, and L. Singer, "Optical under-sampling and reconstruction of several bandwidth-limited signals," *J. Lightwave Technol.* **27**, 1027–1033 (2009).
4. M. B. Airola, S. R. O'Connor, M. L. Dennis, and T. R. Clark, "Experimental demonstration of a photonic analog-to-digital converter architecture with pseudorandom sampling," *IEEE Photon. Technol. Lett.* **20**, 2171–2173 (2008).
5. G. C. Valley, G. A. Sefler, and T. J. Shaw, "Compressive sensing of sparse radio frequency signals using optical mixing," *Opt. Lett.* **37**, 4675–4677 (2012).
6. F. Coppinger, A. Bhushan, and B. Jalali, "Photonic time stretch and its application to analog-to-digital conversion," *IEEE Trans. Microwave Theory Tech.* **47**, 1309–1314 (1999).
7. F. Coppinger, A. Bhushan, and B. Jalali, "Time magnification of electrical signals using chirped optical pulses," *Electron. Lett.* **34**, 399–400 (1998).
8. H. Chi, Y. Chen, Y. Mei, X. Jin, S. Zheng, and X. Zhang, "Microwave spectrum sensing based on photonic time stretch and compressive sampling," *Opt. Lett.* **38**, 136–138 (2013).
9. Y. Chen, H. Chi, T. Jin, S. Zheng, X. Jin, and X. Zhang, "Sub-Nyquist sampled analog-to-digital conversion based on photonic time stretch and compressive sensing with optical random mixing," *J. Lightwave Technol.* **31**, 3395–3401 (2013).
10. B. W. Buckley, A. M. Madni, and B. Jalali, "Coherent time-stretch transformation for real-time capture of wideband signals," *Opt. Express* **21**, 21618–21627 (2013).
11. Y. Han and B. Jalali, "Continuous-time time-stretched analog-to-digital converter array implemented using virtual time gating," *IEEE Trans. Circuits Syst. I, Reg. Papers* **52**, 1502–1507 (2005).
12. M. H. Asghari and B. Jalali, "Anamorphic transformation and its application to time-bandwidth compression," *Appl. Opt.* **52**, 6735–6743 (2013).
13. M. H. Asghari and B. Jalali, "Experimental demonstration of optical real-time data compression," *Appl. Phys. Lett.* **104**, 111101 (2014).
14. J. Chou, O. Boyraz, D. Solli, and B. Jalali, "Femtosecond real-time single-shot digitizer," *Appl. Phys. Lett.* **91**, 161105 (2007).
15. J. Yao, "Photonic generation of microwave arbitrary waveforms," *Opt. Commun.* **284**, 3723–3736 (2011).
16. X. Dong, P. Shum, N. Ngo, C. Chan, J. Ng, and C. Zhao, "A largely tunable CFBG-based dispersion compensator with fixed center wavelength," *Opt. Express* **11**, 2970–2974 (2003).
17. T. Erdogan, "Fiber grating spectra," *J. Lightwave Technol.* **15**, 1277–1294 (1997).
18. J. D. Schwartz, J. Azaña, and D. V. Plant, "Experimental demonstration of real-time spectrum analysis using dispersive microstrip," *IEEE Microwave Wireless Compon. Lett.* **16**, 215–217 (2006).
19. M. A. Laso, T. Lopetegui, M. J. Erro, D. Benito, M. J. Garde, M. A. Muriel, M. Sorolla, and M. Guglielmi, "Real-time spectrum analysis in microstrip technology," *IEEE Trans. Microwave Theory Tech.* **51**, 705–717 (2003).
20. B. Nikfal, S. Gupta, and C. Caloz, "Increased group-delay slope loop system for enhanced-resolution analog signal processing," *IEEE Trans. Microwave Theory Tech.* **59**, 1622–1628 (2011).
21. G. P. Agrawal, *Nonlinear Fiber Optics*, 3rd ed. (Academic, 2001).
22. D. B. Hunter and R. A. Minasian, "Photonic signal processing of microwave signals using an active-fiber Bragg-grating-pair structure," *IEEE Trans. Microwave Theory Tech.* **45**, 1463–1466 (1997).